Study on the Thermal Decomposition Mechanism of Saturated Hydrocarbons in Heavy Oil

Tianfang Yang[1, 2,*], Linsong Cheng[1], Huan Wang[1]

[1]College of Petroleum Engineering, China University of Petroleum-Beijing, Beijing, 102249, China
[2]College of Arts and Sciences, China University of Petroleum-Beijing at Karamay, Beijing, 834000, China

*tfyang@cupk.edu.cn

Abstract. It is of great significance to further investigate the pyrolysis reaction mechanism of heavy oil at various temperatures by simulating the organic model molecular pyrolysis reaction network during heavy oil development. This article employs molecular dynamics simulation methods to examine the high-temperature pyrolysis reaction pathways and networks of heavy oil model molecules (C29H54). The types of reactions, particularly the reaction network at a temperature of 1500 K, were theoretically analyzed through kinetic simulations conducted at different temperatures of 1000 K and 1500 K. This research aims to provide a novel approach for studying the combustion of heavy oil and the conversion of organic molecules at elevated temperatures, as well as to offer recommendations for enhancing the recovery rate of heavy oil.

Keywords: Heavy oil: Reaction pathways; Reaction rate; Reaction netwoks.

1 Introduction

China has extremely abundant heavy oil resources, and how to efficiently develop and utilize heavy oil resources has become an urgent problem that needs to be solved in the upstream and downstream industries of the petroleum industry. Many heavy oil extraction methods have been developed both domestically and internationally, among which steam injection and steam flooding are currently the most commonly used extraction methods in the world[1-2]. Although this method has a good effect on conventional heavy oil, the increase in the production of ultra-heavy oil is relatively small. For ultra-heavy oil, underground upgrading and viscosity reduction technology involves injecting a catalytic viscosity reducer during steam injection. Under the synergistic effect of high-temperature water and catalytic viscosity reducer, the asphaltene and resin in heavy oil undergo cracking, irreversibly reducing the viscosity of heavy oil and improving its quality to a certain extent, thereby reducing its viscosity and making it easy to recover[3-4]. At present, utilizing this technology to extract ultra-heavy oil has become a hot topic of concern.

H. Bilgin et al. (eds.), *Proceedings of the 2024 6th International Conference on Civil Engineering, Environment Resources and Energy Materials (CCESEM 2024)*, Advances in Engineering Research 253,
https://doi.org/10.2991/978-94-6463-606-2_26

In the distribution of heavy oil in China, the characteristics of heavy oil in Karamay, Xinjiang are very prominent. The content of cycloalkanes in heavy oil is as high as 69.7%, and cycloalkane-based heavy oil is known as the "rare earth" in petroleum. The heavy oil in Karamay is the highest quality naphthenic base heavy oil. It is an indispensable rare high-quality raw material for refining aviation kerosene, low pour point diesel oil, ultra-low temperature refrigeration oil, special asphalt, high-end rubber oil, and other special oil products. It has irreplaceable unique value in important industrial fields, major national strategic projects, national defense undertakings, and aerospace projects[5-7]. The study on the reaction mechanism of oxidative cracking of Karamay heavy oil can be of certain significance for the process improvement of viscosity reduction, modification, and catalysis of heavy oil.

2 Methodology

2.1 Simulation Details

Using Materials Studio 8.0 software, models with different numbers of monomers were constructed using the Amorphous Cell module, and energy optimization was performed to make their structure and performance similar to actual materials. Then, molecular dynamics simulations were conducted using the Reaxff force field in the LAMMPS platform[8-14], while using ChemTracy 2.0[15-17].

Analyze the trajectory of the reaction network and gain a deeper understanding of the oxidation cracking mechanism and other processes based on the analysis results.

2.2 Modeling

The modeling and molecular structure of heavy oil systems utilize the molecular structure of heavy oil models provided in reference [5]. The molecular density of heavy oil is 0.9436g/cm3, with a monomer formula of $C_{29}H_{54}$ and a total of 4150 atoms in the system. The cracking temperature is set to 1000K and 1500K.

3 Result and Discussion

3.1 Reaction Mechanism under 1000K Temperature Conditions

From Table 1, it was found that there are 14 reaction paths, mainly isomerization reaction, pyrolysis reaction, and dehydrogenation reaction. The number of isomeric reactions is the highest and the reaction rate is the highest. In the reaction, most reactions are positive, and there are also reverse reactions occurring. Due to the low reaction temperature, the forward reaction is not very active, and the reverse reaction slows down the forward reaction rate.

Table 1. Statistical Table of Reaction Pathways under 1000K Reaction Conditions

R<ID>	Reactions	Rate Constants K (s-1)	N
R0	$C_{29}H_{54}$ -> $C_{29}H_{54}$	4.80×10^{9}	12
R1	$C_{29}H_{54}$ -> $C_{29}H_{54}$	6.40×10^{9}	16
R2	$C_{29}H_{54}$ -> $C_{24}H_{43}$ + C_5H_{11}	2.00×10^{9}	5
R3	$C_{29}H_{54}$ -> $C_{24}H_{43}$ + C_5H_{11}	4.00×10^{8}	1
R4	$C_{29}H_{54}$ -> $C_{29}H_{54}$	2.40×10^{9}	6
R5	$C_{29}H_{54}$ -> $C_{29}H_{54}$	5.60×10^{9}	14
R6	$C_{29}H_{54}$ -> $C_{29}H_{53}$ + H	4.80×10^{9}	12
R7	$C_{29}H_{54}$ -> $C_{29}H_{53}$+ H	4.00×10^{8}	1
R8	$C_{29}H_{54}$ -> $C_{29}H_{53}$ + H	1.60×10^{9}	4
R9	$C_{29}H_{54}$ -> $C_{29}H_{53}$ + H	2.80×10^{9}	7
R10	$C_{29}H_{54}$ -> $C_{29}H_{54}$	1.20×10^{9}	3
R11	$C_{29}H_{54}$ -> $C_{29}H_{54}$	2.00×10^{9}	5
R12	$C_{29}H_{54}$ -> $C_{29}H_{54}$	1.60×10^{9}	4
R13	$C_{29}H_{54}$ -> $C_{29}H_{53}$ + H	4.00×10^{8}	1

Under this condition, the reaction temperature is lower, the types and quantities of products are fewer, and the rate is not high. Only the reaction path is found, and no reaction network is found. From the perspective of reaction times, the reaction paths R0, R1, R4, R5, R10, R11, and R12 are isomeric reactions; R2 and R3 are pyrolysis reactions; R6, R7, R8, R9, and R13 are dehydrogenation reactions.

In isomerization reactions, R1 has the highest reaction rate and the number of times. By analyzing the planar configurations of reactants and products, it is known that the cleavage and ring opening of C-C bonds are involved. Through the analysis of the pyrolysis reaction, it is found that the R2 reaction product is generated by the dissociation of the C-C bond on the ringside chain. The reaction rate and number of times of this reaction are relatively high. In the dehydrogenation reaction, γ-H of the central benzene ring of the reactant dissociates the C-H bond, which gives $C_{29}H_{53}$ some activity[18-20].

3.2 Reaction Mechanism at 1500K Temperature

In the calculation, it was found that there are 34reaction paths, which are isomerization reactions, pyrolysis reactions, and dehydrogenation reactions. The number of isomeric reactions is the highest and the reaction rate is the highest. In the reaction, most reactions are positive, and there are also reverse reactions that occur. Some reaction products (such as free radicals CH_3•, C_2H_5•, H•, etc.) provide conditions for the reaction.

Table 2. Statistical Table of Reaction Pathways under 1500K Reaction Conditions

R<ID>	Reactions	Rate Constants K (s-1)	N
R0	$C_{29}H_{54}$ -> $C_{29}H_{54}$	1.43×10^{12}	1
R1	$C_{29}H_{54}$ -> $C_{29}H_{54}$	9.75×10^{13}	78
R1*	$C_{29}H_{54}$ -> $C_{29}H_{54}$	3.09×10^{10}	77
R2	$C_{29}H_{54}$ -> $C_{29}H_{54}$	4.01×10^{8}	1

R3	$C_{29}H_{54}$ -> $C_{29}H_{54}$	2.45×10^{10}	61
R4	$C_{29}H_{54}$ -> $C_{29}H_{54}$	8.03×10^{8}	2
R5	$C_{29}H_{54}$ -> $C_{29}H_{54}$	2.73×10^{10}	68
R6	$C_{29}H_{54}$ -> $C_{29}H_{53}$ + H	4.01×10^{8}	1
R7	$C_{29}H_{54}$ -> $C_{24}H_{43}$ + C_5H_{11}	2.29×10^{10}	57
R8	$C_{29}H_{54}$ -> $C_{24}H_{43}$ + C_5H_{11}	5.62×10^{9}	14
R9	$C_{29}H_{54}$ -> $C_{29}H_{54}$	3.29×10^{10}	82
R10	$C_{29}H_{54}$ -> $C_{27}H_{49}$ + C_2H_5	4.01×10^{8}	1
R11	$C_{29}H_{54}$ -> $C_{29}H_{53}$ + H	2.01×10^{9}	5
R12	$C_{29}H_{54}$ -> $C_{29}H_{53}$ + H	2.77×10^{10}	69
R13	$C_{29}H_{54}$ -> $C_{29}H_{53}$ + H	6.02×10^{9}	15
R14	$C_{29}H_{54}$ -> $C_{29}H_{53}$ + H	1.61×10^{9}	4
R15	$C_{29}H_{54}$ -> $C_{29}H_{53}$ + H	4.01×10^{8}	1
R16	$C_{29}H_{54}$ -> $C_{29}H_{53}$ + H	3.61×10^{9}	9
R17	$C_{29}H_{54}$ -> $C_{29}H_{53}$ + H	2.41×10^{9}	6
R18	$C_{29}H_{54}$ -> $C_{29}H_{53}$ + H	3.21×10^{9}	8
R19	$C_{29}H_{54}$ -> $C_{29}H_{53}$ + H	2.09×10^{10}	52
R20	$C_{29}H_{54}$ -> $C_{29}H_{53}$ + H	3.61×10^{9}	9
R21	$C_{29}H_{54}$ -> $C_{29}H_{53}$ + H	1.93×10^{10}	48
R22	$C_{29}H_{54}$ -> $C_{29}H_{54}$	1.57×10^{10}	39
R23	$C_{29}H_{54}$ -> $C_{29}H_{54}$	2.97×10^{10}	74
R24	$C_{29}H_{54}$ -> $C_{29}H_{54}$	2.89×10^{10}	72
R25	$C_{29}H_{54}$ -> $C_{29}H_{53}$ + H	5.22×10^{9}	13
R26	$C_{29}H_{54}$ -> $C_{29}H_{53}$ + H	2.81×10^{9}	7
R27	$C_{29}H_{54}$ -> $C_{29}H_{53}$ + H	1.61×10^{9}	4
R28	$C_{29}H_{54}$ -> $C_{29}H_{53}$ + H	2.01×10^{9}	5
R29	$C_{29}H_{54}$ -> $C_{29}H_{53}$ + H	8.03×10^{8}	2
R30	$C_{29}H_{54}$ -> $C_{28}H_{51}$ + CH_3	4.01×10^{8}	1
R31	$C_{29}H_{53}$ + H -> $C_{29}H_{54}$	8.48×10^{11}	1
R31*	$C_{29}H_{54}$ -> $C_{29}H_{53}$ + H		

According to the analysis of Table 2, under 1500K reaction conditions, the isomerization reaction and dehydrogenation reaction have the highest number of reactions. After increasing the reaction temperature, there is a significant increase in reaction type, reaction frequency, and reaction rate. In the reaction, the number of isomerization reactions is the highest, followed by dehydrogenation reactions, pyrolysis reactions are the most frequent, and hydrogenation reactions are the least.

In the isomerization reaction, R1 has the highest number of times and rate, with a reaction rate of $9.75\times10^{13}(S^{-1})$. The structural changes of the reactants and products involve the isomerization of six-membered rings into eight-membered rings after ring opening. Compared with other pyrolysis reactions, R7 has the highest number of reactions and rate, reaching a rate of $2.29\times10^{10}(S^{-1})$. The product $C_5H_{11}\cdot$ of this reaction is produced by the dissociation of the C-C bond on the side chain of the reactant. In the dehydrogenation reaction, the number and rate of R12 reactions are the highest, reaching a rate of $2.77\times10^{10}(S^{-1})$. In the dehydrogenation reaction, the number and rate of

R12 reactions are the highest, reaching a rate of $2.77\times10^{10}(S^{-1})$. The dehydrogenation position of this reaction is at the gamma position on the side ring.

In the above reactions, there are some charged products (CH_3 •, C_2H_5 •, H •) in the generated products, all of which play a role in activating and accelerating the reaction.

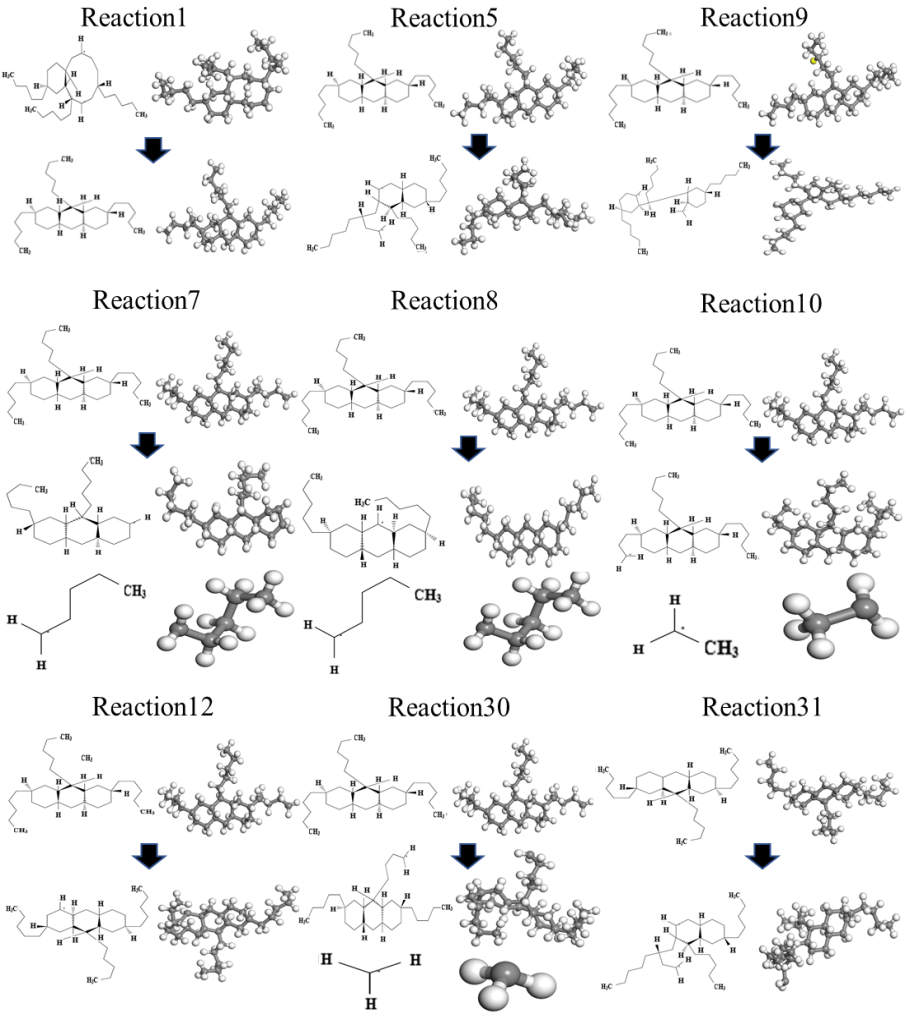

Fig. 1. Reaction Path Diagram

There are many products in the early and late stages of the reaction, with a total of 34 types of products. Isomerization, pyrolysis, and dehydrogenation reactions have a higher frequency and reaction rate. As shown in the Fig.1, using algorithms and graphic recognition, two reaction networks were discovered in 32 reactions, including C-C and C-H bond dissociation, cycloalkane ring opening, and dehydrogenation reactions. During the isomerization reaction in this group, both the opening and closing of cycloalkanes and dehydrogenation reactions occur. As the reaction proceeds, along with the

dissociation of C-C and C-H bonds, isomerization and cleavage reactions occur simultaneously. In the reaction, the generation of free radical molecules accelerates the progress of the reaction, leading to a hydrogenation reaction. Compared with the experiment, it was found that there is a reverse reaction in the reaction network, which is difficult to observe in the experiment.

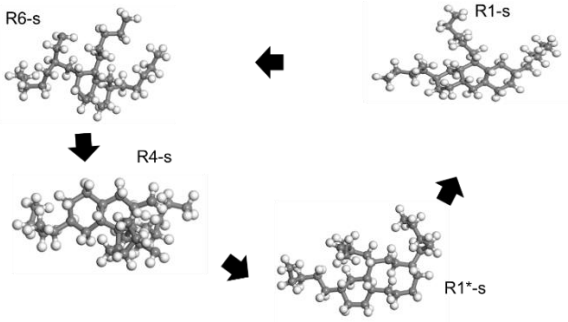

Fig. 2. Schematic diagram of reaction network under 1500K reaction condition. R1-s, R6-s, R4-s, R1*-s represent the products of the reverse reaction of R1, R6, R4, and R1, respectively.

According to the Fig.2, the reaction network is R1-s→ R6-s→R4-s → R1*-s → R1-s. By identifying the reaction network under temperature conditions, it can be seen that in the pyrolysis reaction of $C_{29}H_{54}$, the higher the temperature, the more reaction types and reaction paths there are. The recognition of reaction networks can provide theoretical support for the catalysis of $C_{29}H_{54}$ molecules and the corresponding treatment of heavy oil.

4 Conclusion

The reaction rates of products in pyrolysis reactions vary at different temperatures, the reaction rate and number of reactions at higher temperatures are greater than those at lower temperatures, and there are also many reaction products and types. This can be explained by insufficient contact collisions in the early stage and sufficient reactions in the later stage. The discovery of the reaction network provides a conversion basis for the $C_{29}H_{54}$ reaction and theoretical guidance for further viscosity reduction and enhanced oil recovery of heavy oil. multiple types of reactions were found in the many-reaction pathways, such as dehydrogenation, hydrogenation, and small molecule activation reactions.

Reference

1. Zhao Fulin. Oilfield Chemistry [M]. Dongying: Petroleum University Press, 2003:175-176.
2. Cao Yanbin, Yu Tiantian, Lin Jisheng, et al. Mechanism of improving the development effect of highly sensitive heavy oil reservoirs using thermal composite chemical methods [J]. Journal of Petroleum, 2013, 34 (1): 128-132.

3. Monin J C, Audlbert A, Thermal cracking of heavy oil mineral matrices [R] SPE162691988
4. Clough J. Process for recovering hydrogen: US, 4846274 [P]. 1989-07-11.
5. Tan Ningxin, Wang Jingbo, Hua Xiaoxiao, et al. High-temperature combustion mechanism and kinetic simulation of methylcyclohexane [J]. Journal of Chemistry of Higher Education, 2011, 32 (8) 1832-1937.
6. Cui Qing, Zhang Changqiao, Jianxin, etc Molecular dynamics simulation of viscosity reduction mechanism of heavy oil asphaltene gum [J]. 2017, Journal of Shandong University (Engineering Edition), 2017,47 (2), 123-129.
7. Lei Bin, Huang Juan, Hou Yu, et al. Mechanism of catalytic upgrading and viscosity reduction of Shengli heavy oil [J]. Petrochemical, 2016, 45 (10): 1209-1214.
8. Nikita Orekhov.; Gulnaz Ostroumova.; Vladimir Stegailov.; High temperature pure carbon nanoparticle formation: Validation of AIREBO and ReaxFF reactive molecular dynamics. Carbon, 2020, 270, 606.
9. Döntgen M.; Przybylski-Freund M D.; Kröger L C.; Kopp W A.; Ismail A E.; Leonhard K. Automated discovery of reaction pathways, rate constants, and transition states using reactive molecular dynamics simulations. J. Chem. Theory Comput, 2015, 11, 2517.
10. Döntgen M.; Schmalz F.; Kopp W. A.; Kröger L. C.; Leonhard K. Automated Chemical Kinetic Modeling via Hybrid Reactive Molecular Dynamics and Quantum Chemistry Simulations. J. Chem. Inf. Model. 2018, 58, 1343.
11. Chenoweth, K.; van Duin, A. C. T.; Goddard, W. A. ReaxFFReactive Force Field for Molecular Dynamics Simulations of Hydrocarbon Oxidation. J. Phys. Chem. 2008, 112, 1040−1053
12. Nikita Orekhov.; Gulnaz Ostroumova.; Vladimir Stegailov.; High temperature pure carbon nanoparticle formation: Validation of AIREBO and ReaxFF reactive molecular dynamics. Carbon, 2020, 270, 606.
13. Plimpton, Fast parallel algorithms for short-range molecular dynamics, J. Comput. Phys. 117 (1995) 1–19.
14. H.M. Aktulga, J.C. Fogarty, S.A. Pandit, A.Y. Grama, Parallel reactive molecular
15. Döntgen M.; Przybylski-Freund M D.; Kröger L C.; Kopp W A.; Ismail A E.; Leonhard K. Automated discovery of reaction pathways, rate constants, and transition states using reactive molecular dynamics simulations. J. Chem. Theory Comput, 2015, 11, 2517.
16. Döntgen M.; Schmalz F.; Kopp W. A.; Kröger L. C.; Leonhard K. Automated Chemical Kinetic Modeling via Hybrid Reactive Molecular Dynamics and Quantum Chemistry Simulations. J. Chem. Inf. Model. 2018, 58, 1343.
17. van Duin, A. C. T.; Dasgupta, S.; Lorant, F.;Goddard, W. A., III ReaxFF: a reactive force field for hydrocarbons. J. Phys. Chem. A 2001, 105, 9396−9409.
18. Yuwen Deng.; Wenhao Yuan.; Sandro Gaïl.; Wei Li.; Long Zhao.; Jiuzhong Yang.; Fei Qi.; Yuyang Li.; Philippe Dagaut. Exploration on the combustion chemistry of p-xylene: A comprehensive study over wide conditions and comparison among C8H10 isomers. Combustion and Flame. 2024, 262, 113377.
19. Ding Wancheng, He Lipeng, Geng Xiangfei, et al Study on the Composition and Structure of Ultra Heavy Oil in the Jiu7 District of Xinjiang [J]. Oilfield Chemistry, 2016,33 (3), 516-521.
20. Bin Gui, Qing Y. Yang, Hui J. Wu,† Xin Zhang,† and Yao Lu*, Study of the Effects of Low-Temperature Oxidation on the Chemical Composition of a Light Crude Oil, Energy Fuels 2010, 24, 1139–1145.